Dose-Response:
An International Journal
2018:1-9

DOI: 10.1177/1559325818771527
journals.sagepub.com/home/dos
SAGE

Tumor Cell–Accelerated Senescence Is Associated With DNA-PKcs Status and Telomere Dysfunction Induced by Radiation

Miaomiao Zhang[1,2], Xiaopeng Guo[1,2], Yue Gao[1,2], Dong Lu[1], and Wenjian Li[1]

Abstract

Whether telomere structure integrity is related to radiosensitivity is not well investigated thus far. In this study, we investigated the relation between telomere instability and radiation-induced accelerated senescence. Partial knockdown of DNA-dependent catalytic subunit of protein kinase (DNA-PKcs) in human breast cancer cell line MCF-7 was established by small interfering RNA. Radiosensitivity of control and DNA-PKcs knockdown MCF-7 cells was analyzed by clonogenetic assay. Cell growth was measured by real-time cell electronic sensing. Senescence and apoptosis were evaluated by β-galactosidase histochemical staining and fluorescence-activated cell sorting, respectively. DNA damage was determined by long polymerase chain reaction (PCR). Telomere length and integrity were analyzed by real-time PCR and cytogenetic assay, respectively. DNA-PKcs knockdown MCF-7 cells were more sensitive to X-irradiation than control cells. Further investigation revealed that accelerated senescence is more pronounced than apoptosis in cells after radiation, particularly in DNA-PKcs knockdown cells. The cytogenetic assay and kinetics of DNA damage repair revealed that the role of telomere end-capping in DNA-PKcs, rather than DNA damage repair, was more relevant to radiosensitivity. To our knowledge, this is the first study to show that DNA-PKcs plays an important role in radiation-induced accelerated senescence via maintenance of telomere integrity in MCF-7 cells. These results could be useful for future understanding of the radiation-induced genome instability and its consequences.

Keywords

accelerated senescence, DNA-PKcs, telomere dysfunction, radiation

Introduction

Radiotherapy is used to deprive the tumor cells of their reproductive potential. This can be achieved through programmed cell death, including apoptosis, necroptosis, mitotic catastrophe, and autophagic cell death. However, accumulating evidence suggests that loss of reproductive capacity can occur through an alternative pathway, which has been termed "premature senescence" or "accelerated senescence" (AS).[1] This phenomenon is characterized by the rapid induction of a permanent growth–arrested state with increased granularity and vacuoles, altered morphology, and senescence-associated β-galactosidase activity. Ionizing radiation (IR)-induced AS has been observed in both normal and tumor cells.[2-4] Most solid tumors derived from epithelial cells respond to radiotherapy by senescence rather than apoptosis. Radiation-induced senescence of tumor cells effectively blocks the proliferation of malignant cells and therefore inhibits tumor growth. Understanding the mechanism of IR-induced AS will be important for improving therapies against cancer.

Cellular senescence is associated with telomere dysfunction.[5] Telomeres are specific heterochromatic domains that protect the chromosome ends from unscheduled DNA repair and degradation. The length of telomere repeats and the integrity of telomere-binding proteins are important for the function of telomeres. Although cellular senescence has been associated with telomere attrition and telomerase activity, there is increasing evidence, suggesting that AS induced by IR or antitumor drugs is not

[1] Institute of Modern Physics, Chinese Academy of Sciences, Lanzhou, China
[2] College of Life Science, University of Chinese Academy of Sciences, Beijing, China

Received 11 January 2018; received revised 08 March 2018; accepted 20 March 2018

Corresponding Author:
Dong Lu, Institute of Modern Physics, Chinese Academy of Sciences, Lanzhou, China.
Email: ld@impcas.ac.cn

directly dependent on the length of telomeres. Jones et al reported that AS in response to IR depends on p53 status. They found that IR-induced AS in MCF-7 cells is associated with telomere dysfunction but is unrelated to changes in telomerase activity or telomere lengths.[4] This phenomenon can also be observed in normal human fibroblasts with and without human telomerase reverse transcriptase (hTERT) after irradiation.[6] The lack of direct involvement of telomeres and telomerase in response to radiation can be further addressed by data, suggesting that neither elongated telomeres nor increased telomerase activity serve to protect cells from radiation.[7] However, one cannot ignore the fact that radiation-induced AS accompanies chromosome end–associated abnormalities, including end-to-end fusion (an indicator of telomere dysfunction).[4,8] There is evidence that cellular senescence is induced by the change in the protected status of telomeres rather than by loss of telomeric DNA.[5,9] Therefore, although telomere length is an important trigger for the onset of senescence, the loss of chromosome end protection due to telomere dysfunction may be more important in AS.

In normal cells, telomeres are well protected by the members of shelterin complex, which consists of following 6 main proteins: telomere repeat–binding factor-1 (TRF1), TRF2, TRF1-interacting nuclear protein-2, Ras-related protein-1, tripeptidyl-peptidase-1, and protection of telomeres protein-1.[10] In addition, Bailey et al have revealed that the DNA-dependent protein kinase (DNA-PK) plays an important role in telomere end-capping.[11] Furthermore, they discovered that the catalytic subunit of DNA-PK (DNA-PKcs) is critical for proper telomere end processing and ligase IV is required for uncapped telomere fusion. Uncapped telomeres with DNA-PK deficiency not only misjoin with one another but also inappropriately fuse to IR-induced double-strand breaks (DSBs).[12] A recent report also demonstrated that by selectively knocking down 2 components of DNA-PK, Ku70 and Ku80, in MCF-10A cells, the cellular radiosensitivity increased, which accompanied an increased level of senescence.[13] However, whether DNA-PKcs, the key subunit of DNA-PK, plays a role in IR-induced senescence and its contribution to cellular radiosensitivity remains elusive.

Here, we propose that AS induced by IR may be caused by telomere dysfunction, which is dependent on DNA-PKcs status. We found that compared to MCF-7 cells with normal DNA-PKcs function, MCF-7 cells with DNA-PKcs deficiency exhibit increased radiosensitivity, elevated chromosomal instability, and AS, whereas no significant reduction in the telomere length was observed between the 2. Taken together, our results suggest that telomere dysfunction plays an important role in IR-induced AS, and proteins associated with telomere end-capping are the potential targets for radiotherapy.

Materials and Methods

Cell Culture

The human breast cancer cell line MCF-7 was purchased from the American Type Culture Collection. Cells were maintained in Dulbecco's Modified Eagle's Medium (Sigma St. Louis, MA, USA) supplemented with 10% fetal bovine serum (Hyclone, Logan, UT, USA). Cells were cultured in 5% CO_2 in humidified air at 37°C.

Irradiation Treatment

X-ray was generated with an RX-650 X-ray biological irradiator (FAXITRON, Tucson, AZ,USA) operated at 200 kVp and 20 mA. The dose rates were 1.1 Gy/min. Cells in exponential growth phases were irradiated at room temperature, with non-irradiated culture cells (control) which were handled in parallel with the irradiated samples.

Small Interfering RNA Transfection

Small interfering RNA (siRNA) transfection for the silencing of DNA-PKcs was carried out according to the protocols adapted from Peddi et al.[14] Briefly, MCF-7 cells were trypsinized and washed twice with transfection medium (Santa Cruz Biotechnology, Dallas, TX, USA) before the initiation of the transfection procedure. Twenty-four microliters of siRNA–DNA-PKcs or control siRNA duplex (Santa Cruz Biotechnology) was mixed with 200 μL of transfection medium in a microcentrifuge tube and incubated for 5 minutes at room temperature (RT). During the same time, 24 μL of transfection reagent (Santa Cruz Biotechnology) was mixed with 200 μL of transfection medium in a separate microcentrifuge tube and incubated for 5 minutes at RT. The solutions in these separate microcentrifuge tubes were mixed, incubated for 30 minutes and then mixed with cells (1×10^6cells) suspended in 1.6 mL of transfection medium. The cells were plated onto a 25 cm^2 flask, and after 7 hours of incubation at 37°C, 2 mL of fresh normal medium was added and the cells were further incubated for 24 hours before this medium was replaced with fresh medium. siRNA–DNA-PKcs transfection was repeated in the same way 3 days after the initial transfection (second transfection). Western blotting was performed on day 3 after the second transfection to check the efficacy of transfection.

Immunoblotting

For the preparation of whole cell lysates, cells were washed twice with phosphate-buffered solution (PBS). In the resulting cell pellet, 500 μL of lysis buffer (25 mM Tris, 250 mM NaCl, 1 mM phenylmethylsulfonyl fluoride) supplemented with protease inhibitors (complete protease inhibitor cocktail; Roche Applied Science, Nutley, New Jersey) was added and incubated on ice for 30 minutes. Cell suspension was then sonicated and centrifuged at 14 000 × g. Protein in the supernatant was quantified using the standard Bradford assay (BioRad, Hercules, California). Approximately 25 μg of whole cell protein was mixed with an equal quantity of 2× sodium dodecyl sulfate (SDS) buffer (2.5% SDS, 5.0% β-mercaptoethanol), boiled for 10 minutes, and placed on ice. Protein was loaded onto a 4% to 20% Tris–HCl gradient gel (BioRad) along with

5 μL of Kaleidoscope marker (BioRad). Ice-cold running tank buffer (250 mM Tris, 1.91 M glycine, 34 mM SDS, pH 8.3) was poured into the apparatus and maintained at a temperature of ~4°C. The gel was run at 180 V and 70 mA for 90 minutes using constant voltage. polyvinylidene fluoride (PVDF) membrane (Millipore, Billerica MA USA) was prepared by placing it in 100% methanol for 20 seconds, followed by washing in double distilled water for 2 minutes, and finally placing it in transfer buffer (200 mM glycine, 25 mM Tris, 10% methanol, pH 8.3) for acclimation. A transfer program 150 V, 400 mA, 12 hours was used to transfer the proteins onto the membrane at 4°C. After protein transfer, PVDF membrane was soaked in methanol for 30 seconds and then allowed to dry at RT for 10 minutes. The dried membrane was then placed in blocking solution (tris buffed saline, [TBS] milk: 5% nonfat dry milk in 1× TBS) and allowed to incubate for 1 hour at RT. Membrane was then briefly washed using 1× TBS (10 mM Tris–HCl; 150 mM NaCl, pH 8.0) for 10 minutes and then incubated with a 1:250 dilution of mouse polyclonal DNA-PKcs primary antibody (Santa Cruz Biotechnology) overnight on a rocker and incubated at 4°C. For immunodetection, PVDF membrane was washed with tris buffed saline tween (TBST) (10 mM Tris–HCl; 150 mM NaCl, pH 8.0, and 0.5% Tween-20) for 1 hour with buffer changes every 10 minutes and transferred to fresh TBS buffer containing goat anti-mouse HRP secondary antibody (Pierce, Rockford, Illinois) at a dilution of 1:2000 and incubated at RT for 1 hour. Numerous washes were then given to the membrane using TBST buffer for 1 hour. Protein was detected by chemiluminescence by adding the SuperSignal West Pico Chemiluminescent Substrate (Pierce) to the blot and incubating for 2 minutes. A digital image was obtained using a FluorChem 8800 imaging system (Alpha Innotech Corporation, San Leandro, California). Electronic images were then processed using QuantiScan (BioSoft, Cambridge, United Kingdom) in order to evaluate the DNA-PKcs levels for each cell line as band total intensity. Cells with DNA-PKcs level <20% compared to that of mock-transfected cells were used for further analysis.

Clonogenic Assay

Cells in exponential growth were seeded in Petri dishes (5 cm diameter) for colony formation. For cells that were not subjected to radiation and for those exposed to the low radiation doses used (up to 3 Gy), 1500 cells were seeded in each dish, yielding an adequate countable number of colonies for the respective cell lines after approximately 2 weeks. In the experiments with higher radiation doses (up to 4 or 6 Gy), 3000 or 6000 cells were seeded in each dish, respectively, for both cell lines. Radiation was given 4 hours after the cells were seeded. At this time, the cells were attached to the bottom of the dish but had not yet been able to divide. Cells were further incubated until the colonies formed were large enough to be counted, while still being separable. Owing to the small numbers of cells in the dishes, it was not necessary to change medium during the incubation period. The colonies were then fixed with methanol (3 minutes) and stained with 0.6% Giemsa solution (Giemsa azur-eosin-methylene blue (Merck, Darmstadt, Germany) dissolved in water:methanol solution of 1:1). The colonies were counted manually. Only colonies containing more than about 50 cells were scored.

Apoptosis Assay

For apoptosis assay, propidium iodide (PI; Sigma, Shanghai, China) was used. The cells were trypsinized, washed twice with cold PBS, fixed with 70% ethanol in PBS for 30 minutes, and then stained with a solution containing 5 μg/mL PI, 10 kU/mL RNase (Sigma), and 0.005% Triton-100 in the dark for 30 minutes at RT before flow cytometric analysis. Sub-G1 content was scored as apoptotic cells. The samples were detected with fluorescence-activated cell sorting Calibur (Becton, Dickinson and Company, CA, USA). Unstained cells were analyzed as controls and used to gate on live cells for final analysis. A minimum of 10 000 cells analyzed in each sample served to determine the apoptotic cells using Flowjo 7.2.1 software. Three independent experiments were performed.

Senescence Assay

β-Galactosidase histochemical staining MCF-7 cells were washed twice with PBS and fixed with 2% formaldehyde, 0.2% glutaraldehyde for 5 minutes. The cells were then washed again with PBS and stained with a solution of 1 mg/mL 5-bromo-4-chloro-3-inolyl-β-galactosidase in dimethylformamide (20 mg/mL stock). Following overnight incubation at 37°C, the cells were washed twice with PBS, and the percentage of positively stained cells was determined after counting 3 random fields of 100 cells each. Representative microscopic fields were photographed under a ×40 objective.

Cell Growth Measurements by Real-Time Cell Electronic Sensing System

The real-time cell electronic sensing (RT-CES) system has been described previously.[15,16] For time-dependent cell response profiling, 100 μL of media was added to 96-well E-plates to obtain background readings followed by the addition of 100 μL of cell suspension. The E-plates containing the cells were allowed to incubate at RT for 30 minutes and placed on the reader in the incubator for continuous recording of impedance as reflected by cell index. After 14 hours, the cells were treated with 4 Gy X-ray irradiation. The cells were monitored every 2 hours for the duration of 124 hours to capture the long-term response.

Measurement of DSBs Repair

As PNA-PKcs plays an important role in the nonhomologous end-joining (NHEJ) pathway of DNA damage repair, the kinetics of DNA damage repair was evaluated by long polymerase chain reaction (PCR) assay. Long PCR for the evaluation of mtDNA damage was performed using the GeneAmp XL

Table 1. Characterization of Cytogenetic Abnormalities in MCF-7 Cells After Irradiation.

Cell Line	Metaphases Scored	Metaphases With Abnormalities	Chromosome/ Chromatid Fusions	Chromosome/ Chromatid Breaks
Mock-siRNA	50	6	2	4
DNA-PKcs siRNA	50	41	36	6

Abbreviations: DNA-PKcs, DNA-dependent catalytic subunit of protein kinase; siRNA, small interfering RNA.

PCR kit (PerKin–Elmer, Boston, MA, USA) according to the protocol described previously.[17,18] Quantitative long PCR was performed in an Eppendorf Mastercycler PCR system (Eppendorf, Hamburg, Germany). The PCR cycle test was performed before to ensure the PCR is in the exponential phase. The sequence information of the primers is listed in Table 1. The hot-start PCR was initiated with an addition of the polymerase when the reaction temperature reached 75°C and was performed with following conditions: an initial denaturation for 1 minute at 94°C, followed by 25/20 cycles for large/small fragments of 94°C denaturation for 15 seconds and 68°C extension for 15 minutes. A final extension at 72°C was performed for 10 minutes. An aliquot of each PCR product was resolved on a 1% vertical agarose gel and electrophoresed in Tris–borate–EDTA for 4 hours. The gels were then digitally photographed and quantified with FluorChem FC2 (Alpha Innotech Corporation). The DNA damage was quantified by comparing the relative level of amplification of the large fragments of DNA (10.4-kb *HPRT* gene) normalized to the amplification of smaller (107-bp actin) fragments.

Quantitative PCR for Telomere Length Measurement

The LightCycler 2.0 System (Roche Molecular System, Alameda, California) was used for quantitative PCR analysis. Total genomic DNA (50 ng) was used for telomere length assay in a 20-μL reaction containing 1X SYBR Premix Ex Taq II (TaKaRa, Japan) and 200 nmol/L each primer. The sequence information regarding the primers is listed in Table 1. Triplicate reactions were performed for each marker in 20 μL capillary using the following thermal cycling profile adapted from Cawthon[19]: 15 minutes at 95°C at stage 1; 2 cycles for 15 seconds at 94°C, 15 seconds at 49°C at stage 2; 32 cycles for 15 seconds at 94°C, 10 seconds at 62°C, 15 seconds at 74°C with signal acquisition at stage 3. The signals obtained at 74°C provided the Ct values for the amplification of the telomere and actin template. Relative quantification approach (ΔΔCt) was used according to the method previously described.[20] Each test was carried out in triplicate.

Cytogenetic Analysis

Metaphase chromosomes were harvested from the MCF-7 cell cultures using standard methods. Actively dividing cells were blocked in mitosis with 0.1 μg/mL colcemid for 2 hours, incubated in hypotonic solution (0.075 M KCl) for 20 minutes, and fixed in methanol:glacial acetic acid (3:1). Slides were made using standard procedures, and metaphase chromosomes were visualized using conventional Giemsa staining. Metaphase spreads were scored for chromosomal findings from both the siRNA-mock MCF-7 and DNA-PKcs siRNA MCF-7 cell cultures before and after IR. A total of 100 metaphase spreads (50 each) were evaluated.

Statistical Analysis

Statistical analysis was performed on the means of the data obtained from at least 3 independent experiments. Data are presented as means (standard deviation). Student *t* test was used to detect statistical significance. $P < .05$ was considered to be statistically significant. Microsoft Excel was used for statistical analysis.

Results

As shown in Figure 1, the efficient knockdown for DNA-PKcs was achieved after 2 successive siRNA transfections (3 days apart). Western blotting was performed for the quantitation of these results (Figure 1). Western blot analyses showed a significant inhibitory effect of siRNA on DNA-PKcs expression at day 3 post–double transfection. The DNA-PKcs protein levels in cells on the third day after second transfection were significantly less (<20% of mock-transfected cells) compared to the protein levels in mock-transfected cells.

The radiosensitivity of the cells was examined by a clonogenic assay. As illustrated in Figure 2, the radiosensitivity of DNA-PKcs-deficient cells was greater than that of control and mock MCF-7 cells. These data also showed that the radiosensitivity was similar in control and mock MCF-7 cells. Real-time monitoring of the growth and proliferation of 3 cell lines after radiation was achieved using the RT-CES platform. Figure 2 shows the time-dependent growth and proliferation of 3 cell lines in the E-plates. The growth of siRNA-MCF-7 cells after radiation was significantly suppressed as compared to that of the MCF-7 and mock-siRNA MCF-7 cell lines. No significant difference was observed in growth and proliferation between MCF-7 and mock-siRNA MCF-7 with or without radiation.

The enhanced radiosensitivity may depend on apoptosis or senescence. Therefore, apoptosis and senescence were investigated in both control (siRNA mock-transfected) and DNA-PKcs knockdown MCF-7 cells (Figures 3 and 4). Less than

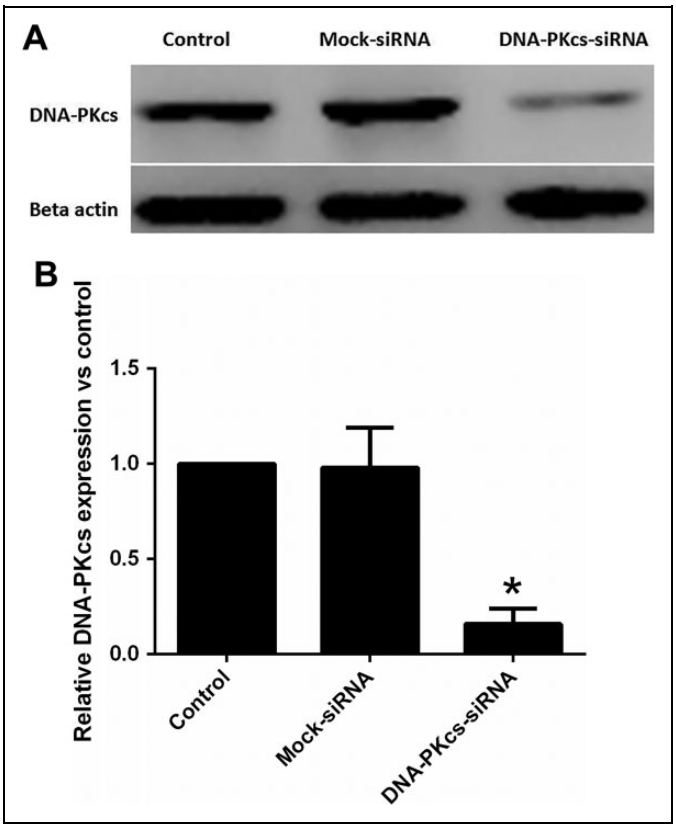

Figure 1. Silencing of DNA-PKcs expression in MCF-7 cells after transfection with siRNA targeted to knockdown the expression of *Prkdc* gene. A, Western blotting showing reduced expression of DNA-PKcs protein in siRNA DNA-PKcs double transfected MCF-7 cells. MCF-7 cell lysates were prepared on 3 days after the second transfection from transfected and mock-transfected (control siRNA only) cells. Twenty-five microgram of protein was loaded in each lane and probed using rabbit polyclonal antibody against DNA-PKcs and mouse monoclonal antibody against β-actin used as standard. B, Quantitation of immunoblotting results. DNA-PKcs band total intensity of control MCF-7 has been used for control and all values were normalized to that. Values are averages from 3 independent experiments. Error bars, SEM. *Statistical significant at $P < .05$. DNA-PKcs indicates DNA-dependent catalytic subunit of protein kinase; SEM, standard error of the mean; siRNA, small interfering RNA.

2% of apoptotic/necrotic cells were detected after irradiation in both cell lines by annexin/PI double staining. In addition, the number of apoptotic cells were relatively low in both cells after X-irradiation as measured by sub-G1 assay (8.46% [0.24%] and 6.48% [0.26%] apoptotic cells, respectively). Overall, the apoptotic response to radiation was very limited in both cell lines. Although no significant change in the number of apoptotic cells was evident between the 2 cell lines 48 hours after 4 Gy irradiation, more than 2-fold increase in cellular senescence was observed in DNA-PKcs-deficient cells. Taken together, AS played a dominant role in radiation-induced tumor inhibition.

Telomere lengths are a critical factor for the onset of cellular senescence. To investigate whether senescence induced by radiation is due to a reduction in the telomere lengths, a modified real-time PCR was used. Results showed that there is no significant reduction in telomere lengths in both cell lines after radiation. Note that telomeres in DNA-PKcs-deficient cells were not significantly shorter than those in the control at the time when AS is pronounced (5 days after irradiation). Therefore, the increase in AS is not related to a reduction in the telomere lengths (Figure 5). Next, we examined the chromosome aberration in control and DNA-PKcs-deficient MCF-7 cells. There was a significant increase in chromosome/chromatid fusions in DNA-PKcs-deficient cells, as compared to that in the control cells (Table 1). These fusions, which are indicative of telomere instability, suggest that DNA-PKcs deficiency is strongly associated with radiation-induced telomere instability.

An important role of DNA-PKcs is its involvement in DNA damage repair. As shown in Figure 5, the relative amplification of hypoxanthine-guanine phosphoribosyltransferase HPRT fragment significantly decreased within 12 hours postirradiation. For the control cells, the relative amplification was restored almost to background levels within 48 hours, whereas for the DNA-PKcs-deficient cells, the relative amplification was still below the control level 48 hours postirradiation ($\sim$88% vs the control levels). There was a statistically significant difference between the 2 cell lines regarding the PCR amplification at all-time point's 48 hours postirradiation ($P < .05$). For each time point within 48 hours postirradiation, the PCR amplification was always lower for DNA-PKcs-deficient MCF-7 (statistically significant difference for 4, 12, 24, and 48 hours, $P < .05$). The reduced amplification even 24 hours postirradiation (especially for siRNA MCF-7) indicated incomplete DNA repair in both cell lines, but significantly more damage in the DNA-PKcs-deficient cells. The data revealed a significant reduction in the capacity of DNA damage repair for the deficient MCF-7 cells; however, DNA damage in both cells was eventually repaired in 72 hours. At this time point, AS is not significant evident although morphological change can be observed (data not shown). Therefore, reduced DNA damage repair caused by DNA-PKcs deficiency may not be the main cause of AS induction.

Discussion

Clonogenic assay is universally recognized as the gold standard for measuring the effects of radiation on cell viability. However, whether reduced cell viability is caused by cell death (apoptosis or necrosis) or by permanent cell growth arrest (cellular senescence) remains to be further investigated. A previous study showed that radiosensitivity is not solely dependent on deregulated apoptosis.[21] Cells after irradiation may proceed rapidly to cell death through apoptosis, necrosis, autophagy, or mitotic catastrophe.[22-25] If survived, cells may undergo growth arrest for DNA damage repair. However, delayed apoptosis or mitotic catastrophe may occur upon reentry into the cell cycle. In addition, permanent cell cycle arrest, such as AS, can be induced in cells over a prolonged period of time after IR.[2,8,26] In our study, 4 to 6 Gy X-irradiation did not result in

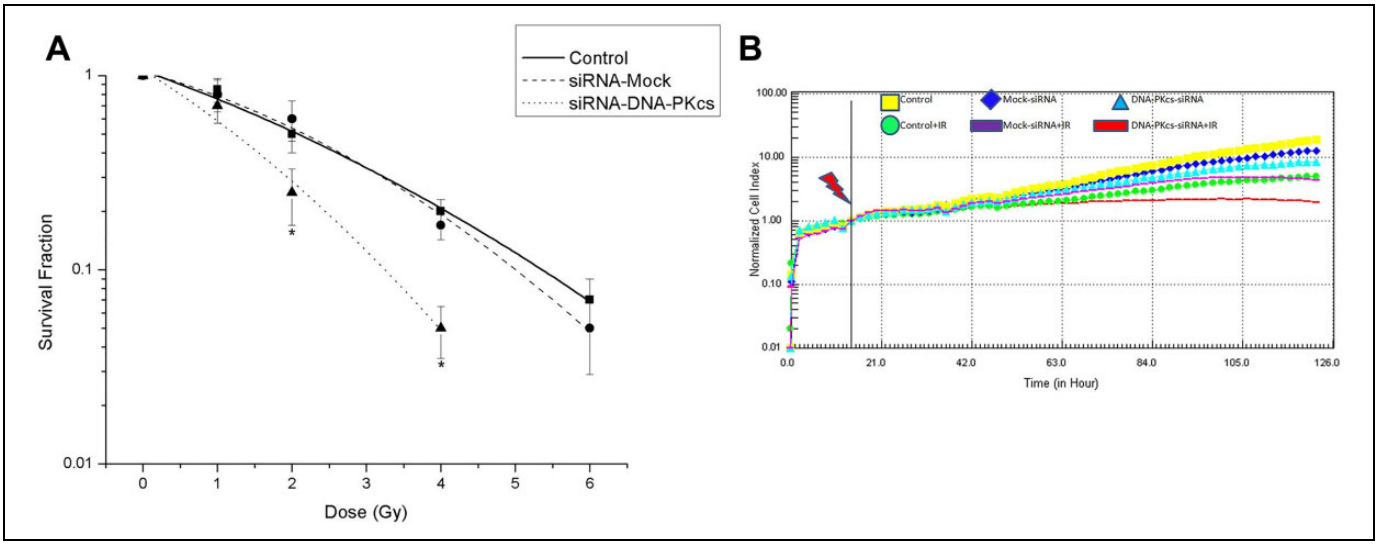

Figure 2. Effect of DNA-PKcs on the sensitivity of MCF-7 cells to ionizing radiation. A, Cell survival was assessed using a colony-formation assay. The surviving fraction was corrected for cell survival in the absence of radiation. Values represent the mean of triplicate determinations. Error bars, SEM. *Statistical significant at $P < .05$ compared to control. B, Real-time monitoring of adherent cells by the RT-CES system. Real-time monitoring of the growth and proliferation of 3 cell lines on the RT-CES platform. The cells suspensions were transferred to E-plates and placed on the RT-CES reader for real-time monitoring every 2 hours for the duration of the assay. The flash arrow indicates the point of 4 Gy radiation. DNA-PKcs indicates DNA-dependent catalytic subunit of protein kinase; SEM, standard error of the mean; RT-CES, real-time cell electronic sensing.

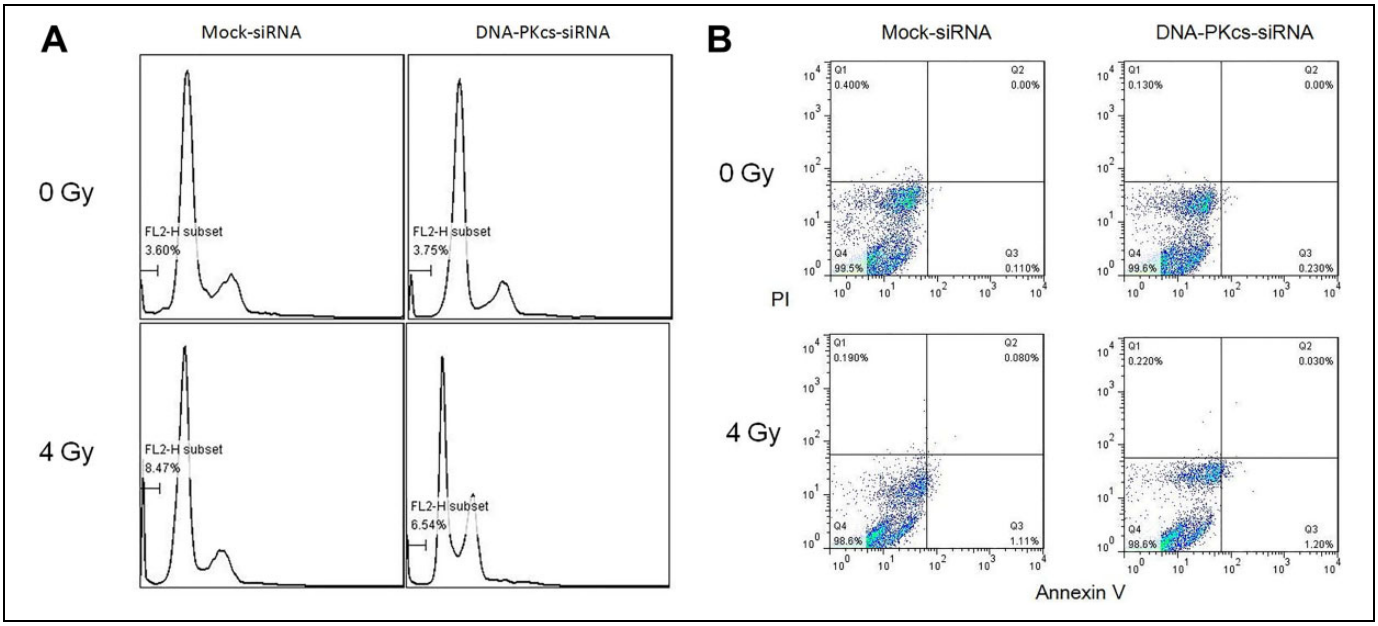

Figure 3. Apoptosis induced by X-irradiation in DNA-PKcs knockdown and control cells. Cells were irradiated with 4 Gy X-ray. Apoptosis was assessed 48 hours after radiation treatment. A, Representative images of sub-G1 population in different cell lines 48 hours after 4 Gy irradiation. B, Representative images of annexin V/PI double staining in different cell lines 48 hours after 4 Gy irradiation. DNA-PKcs indicates DNA-dependent catalytic subunit of protein kinase; PI, propidium iodide.

obvious decrease in cell vitality tested by methyl thiazolyl tetrazolium MTT assay after 72 hours, which significantly reduced clonogenic survival in MCF-7 cells (data not shown). Therefore, cell death, such as apoptosis, may not be the leading cause of inhibition of cellular proliferation induced by IR in MCF-7 cells. In agreement with Gewirtz et al's findings,[4] here we demonstrated that the radiosensitivity of MCF-7 cells was mainly determined by radiation-induced AS but not apoptosis. This was verified using DNA-PKcs-deficient MCF-7 cells. Cell growth was markedly inhibited in DNA-PKcs-deficient cells after irradiation, suggesting that DNA-PKcs may play an important role in radiosensitivity.

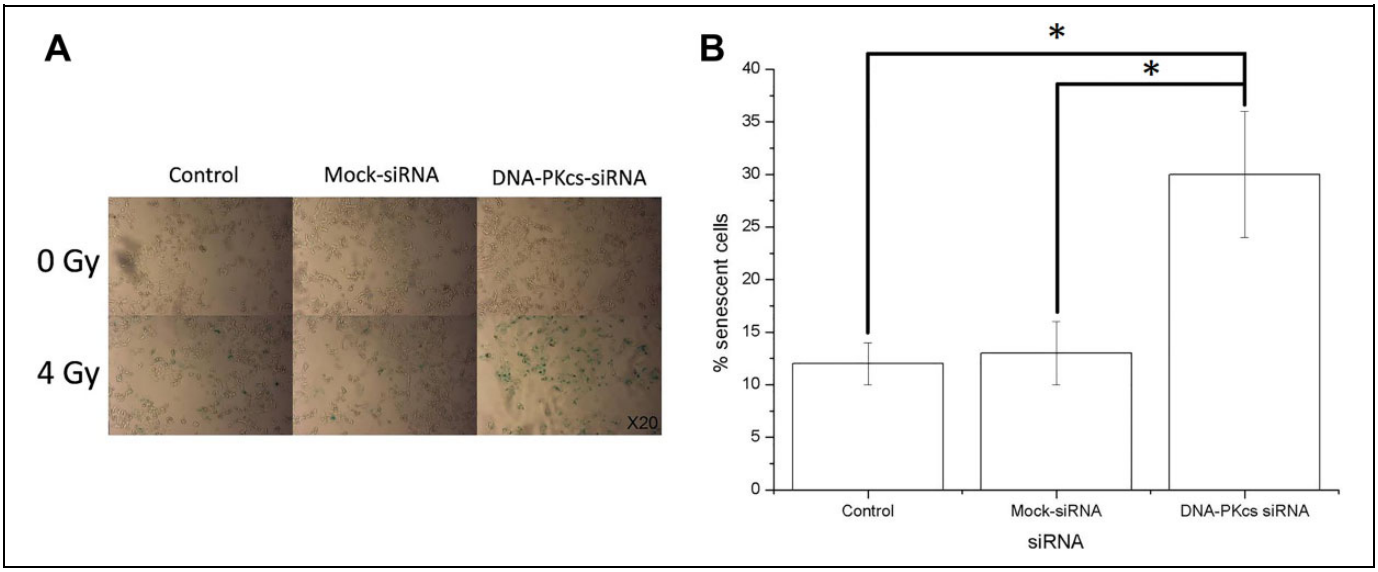

Figure 4. Expression of senescence-associated β-galactosidase in MCF-7 DNA-PKcs knockdown and control cells after irradiation. Cells were irradiated with 4 Gy X-ray, and β-galactosidase expression was assessed 5 days after radiation treatment. A, Representative microscopic fields from untreated (upper panel) and radiation-treated (lower panel) cells. Original magnification for both cells is ×20. Note the substantial increase in cellular volume and the blue staining of the treated cells, especially in DNA-PKcs-deficient MCF-7 cells. B, Quantitation of radiation-induced senescent cells. Values are averages from 3 independent experiments. Error bars, SEM. DNA-PKcs indicates DNA-dependent catalytic subunit of protein kinase; SEM, standard error of the mean.

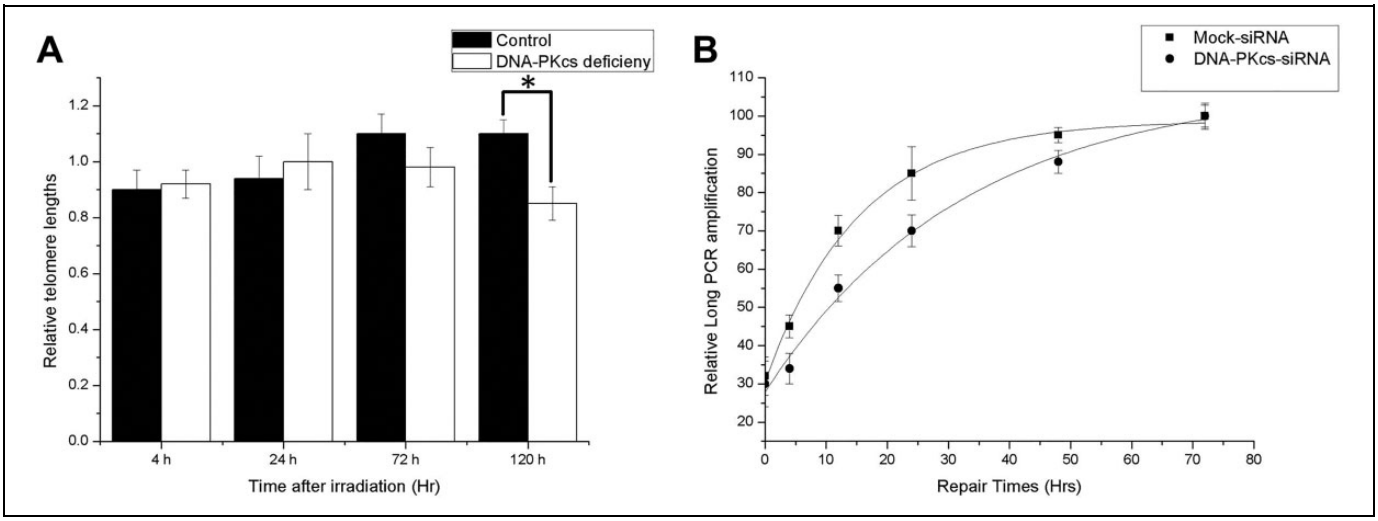

Figure 5. Telomere lengths and processing of DNA damage repair in MCF-7 DNA-PKcs knockdown and control cells after irradiation. A, Cells were irradiated with 4 Gy X-ray, and telomere lengths were assessed 0 to 5 days after radiation by a modified real-time PCR approach. Relative data are expressed as mean value versus nonirradiated control. Values are averages from 3 independent experiments. Error bars, SEM. B, Kinetics of DNA damage repair in siRNA MCF-7 and control (mock-transfected) cells after exposure to 4 Gy of X-rays. Quantitative data for the long PCR amplification expressed as total mean intensity versus nonirradiated control. Values are averages from 3 independent experiments. Error bars, SEM; closed symbols, siRNA MCF-7 cells. Open symbols, control MCF-7 cells. *Statistical significant at $P < .05$. DNA-PKcs, DNA-dependent catalytic subunit of protein kinase; PCR, polymerase chain reaction; SEM, standard error of the mean; siRNA, small interfering RNA.

DNA-PKcs deficiency could cause downregulation of ataxia telangiectasia-mutated gene ATM[27] and γH2AX[28] as well as in impaired phosphorylation of proteins involved in DNA repair and checkpoint.[29] Therefore, using focus assays, such as γH2AX or 53bp1, may not be an appropriate choice to distinguish the difference between wild-type MCF-7 cells and DNA-PKcs-deficient cells. Using long PCR assay, which is entirely based on the damage of DNA strands, we found that DNA damage induced by radiation in DNA-PKcs-deficient cells was repaired slower than in wild-type MCF-7 cells. However, DNA damage in both cell lines was eventually repaired within 72 hours. One of the differences was that chromosome aberrations

were significantly increased in DNA-PKcs-deficient MCF-7 cells. The increase in chromosome fusions may be directly caused by DNA-PKcs deficiency owing to its critical role in telomere end-capping.

DNA-PKcs is required for the NHEJ pathway of DNA repair. Recent studies also show that DNA-PKcs is involved in telomere end protection. Uncapped telomeres in DNA-PKcs-deficient backgrounds may erroneously fuse to IR-induced DSBs, resulting in genome instability. The relation between telomere dysfunction and DNA-PKcs deficiency has been well studied by Bailey et al.[11,30] They demonstrated that uncapped telomeres with DNA-PKcs are inappropriately detected and progressed as DSBs, and thus participated in IR-induced telomere–DSB fusion events. In accordance with their model, we found significant increase in chromosome fusions in DNA-PKcs-deficient MCF-7 cells after irradiation.

The potential impact of cytogenetic aberrations on the response of tumor cells to radiation has not been extensively studied. Here we showed that the increased chromosome fusion, which was caused by telomere dysfunction, accompanied elevated AS in DNA-PKcs-deficient MCF-7 cells. Previous reports suggest that increased telomere dysfunction, rather than telomere length, results in the induction of the senescent state.[5,31] Using a modified real-time PCR assay, we detected no obvious telomere length alteration in both cell lines after X-irradiation in short time. Therefore, using DNA-PKcs-deficient and wild-type MCF-7 cells, we provide further evidence supporting the finding that telomere dysfunction, but not telomere length, is one of the causal factor of IR-induced AS.

In conclusion, we found that AS plays a dominant role in determining the cellular radiosensitivity rather than apoptosis in MCF-7 cells. Our findings provide evidence that telomere dysfunction caused by DNA-PKcs deficiency could influence radiosensitivity by inducing AS.

Declaration of Conflicting Interests

The author(s) declared no potential conflicts of interest with respect to the research, authorship, and/or publication of this article.

Funding

The author(s) disclosed receipt of the following financial support for the research, authorship, and/or publication of this article: This study was funded by the Joint project of Chinese Academy of Sciences and Industrial Technology Research Institute (CAS-ITRI 201705).

References

1. Gewirtz DA, Holt SE, Elmore LW. Accelerated senescence: an emerging role in tumor cell response to chemotherapy and radiation. *Biochem Pharmacol*. 2008;76(8):947-957.
2. Suzuki K, Mori I, Nakayama Y, Miyakoda M, Kodama S, Watanabe M. Radiation-induced senescence-like growth arrest requires TP53 function but not telomere shortening. *Radiat Res*. 2001; 155(1 pt 2):248-253.
3. Podtcheko A, Namba H, Saenko V, et al. Radiation-induced senescence-like terminal growth arrest in thyroid cells. *Thyroid*. 2005;15(4):306-313.
4. Jones KR, Elmore LW, Jackson-Cook C, et al. p53-Dependent accelerated senescence induced by ionizing radiation in breast tumour cells. *Int J Radiat Biol*. 2005;81(6):445-458.
5. Karlseder J, Smogorzewska A, de Lange T. Senescence induced by altered telomere state, not telomere loss. *Science*. 2002; 295(5564):2446-2449.
6. Gorbunova V, Seluanov A, Pereira-Smith OM. Expression of human telomerase (hTERT) does not prevent stress-induced senescence in normal human fibroblasts but protects the cells from stress-induced apoptosis and necrosis. *J Biol Chem*. 2002; 277(41):38540-38549.
7. Rubio MA, Kim SH, Campisi J. Reversible manipulation of telomerase expression and telomere length. Implications for the ionizing radiation response and replicative senescence of human cells. *J Biol Chem*. 2002;277(32):28609-28617.
8. Zahnreich S, Melnikova L, Winter M, et al. Radiation-induced premature senescence is associated with specific cytogenetic changes. *Mutat Res*. 2010;701(1):60-66.
9. O'Sullivan RJ, Karlseder J. Telomeres: protecting chromosomes against genome instability. *Nat Rev Mol Cell Biol*. 2010;11(3): 171-181.
10. de Lange T. Shelterin: the protein complex that shapes and safeguards human telomeres. *Genes Dev*. 2005;19(18):2100-2110.
11. Bailey SM, Meyne J, Chen DJ, et al. DNA double-strand break repair proteins are required to cap the ends of mammalian chromosomes. *Proc Natl Acad Sci U S A*. 1999;96(26):14899-14904.
12. Bailey SM, Cornforth MN, Ullrich RL, Goodwin EH. Dysfunctional mammalian telomeres join with DNA double-strand breaks. *DNA Repair (Amst)*. 2004;3(4):349-357.
13. Vandersickel V, Mancini M, Marras E, et al. Lentivirus-mediated RNA interference of Ku70 to enhance radiosensitivity of human mammary epithelial cells. *Int J Radiat Biol*. 2010;86(2):114-124.
14. Peddi P, Francisco DC, Cecil AM, Hair JM, Panayiotidis MI, Georgakilas AG. Processing of clustered DNA damage in human breast cancer cells MCF-7 with partial DNA-PKcs deficiency. *Cancer Lett*. 2008;269(1):174-183.
15. Atienza JM, Yu N, Kirstein SL, et al. Dynamic and label-free cell-based assays using the real-time cell electronic sensing system. *Assay Drug Dev Technol*. 2006;4(5):597-607.
16. Solly K, Wang X, Xu X, Strulovici B, Zheng W. Application of real-time cell electronic sensing (RT-CES) technology to cell-based assays. *Assay Drug Dev Technol*. 2004;2(4):363-372.
17. Yakes FM, VanHouten B. Mitochondrial DNA damage is more extensive and persists longer than nuclear DNA damage in human cells following oxidative stress. *Proc Natl Acad Sci U S A*. 1997; 94(2):514-519.
18. Worgul BV, Medvedovsky C, Powers-Risius P, Alpen E. Accelerated heavy ions and the lens. IV. Biomicroscopic and cytopathological analyses of the lenses of mice irradiated with 600 MeV/amu 56Fe ions. *Radiat Res*. 1989;120(2):280-293.
19. Cawthon RM. Telomere length measurement by a novel monochrome multiplex quantitative PCR method. *Nucleic Acids Res*. 2009;37(3):e21.
20. Kantor AF, Li FP, Janov AJ, Tarbell NJ, Sallan SE. Hypertension in long-term survivors of childhood renal cancers. *J Clin Oncol*. 1989;7(7):912-915.

21. Enns L, Barley RD, Paterson MC, Mirzayans R. Radiosensitivity in ataxia telangiectasia fibroblasts is not associated with deregulated apoptosis. *Radiat Res*. 1998;150(1):11-16.
22. Kodym E, Kodym R, Choy H, Saha D. Sustained metaphase arrest in response to ionizing radiation in a non-small cell lung cancer cell line. *Radiat Res*. 2008;169(1):46-58.
23. Eriksson D, Lofroth PO, Johansson L, Riklund KA, Stigbrand T. Cell cycle disturbances and mitotic catastrophes in HeLa Hep2 cells following 2.5 to 10 Gy of ionizing radiation. *Clin Cancer Res*. 2007;13(18 pt 2):5501s-5508s.
24. Mendonca MS, Chin-Sinex H, Dhaemers R, Mead LE, Yoder MC, Ingram DA. Differential mechanisms of x-ray-induced cell death in human endothelial progenitor cells isolated from cord blood and adults. *Radiat Res*. 2011;176(2):208-216.
25. Lee SJ, Choi SA, Lee KH, et al. Role of inducible heat shock protein 70 in radiation-induced cell death. *Cell Stress Chaperones*. 2001;6(3):273-281.
26. Richardson RB. Ionizing radiation and aging: rejuvenating an old idea. *Aging (Albany NY)*. 2009;1(11):887-902.
27. Peng Y, Woods RG, Beamish H, et al. Deficiency in the catalytic subunit of DNA-dependent protein kinase causes down-regulation of ATM. *Cancer Res*. 2005;65(5):1670-1677.
28. An J, Huang YC, Xu QZ, et al. DNA-PKcs plays a dominant role in the regulation of H2AX phosphorylation in response to DNA damage and cell cycle progression. *BMC Mol Biol*. 2010;11:18.
29. Callen E, Jankovic M, Wong N, et al. Essential role for DNA-PKcs in DNA double-strand break repair and apoptosis in ATM-deficient lymphocytes. *Mol Cell*. 2009;34(3):285-297.
30. Williams ES, Klingler R, Ponnaiya B, et al. Telomere dysfunction and DNA-PKcs deficiency: characterization and consequence. *Cancer Res*. 2009;69(5):2100-2107.
31. Elmore LW, Rehder CW, Di X, et al. Adriamycin-induced senescence in breast tumor cells involves functional p53 and telomere dysfunction. *J Biol Chem*. 2002;277(38):35509-35515.